

Weather conditions conducive to Beijing severe haze more frequent under climate change

Wenju Cai^{1,2}, Ke Li^{3,4}, Hong Liao^{5*}, Huijun Wang⁶ and Lixin Wu¹

The frequency of Beijing winter severe haze episodes has increased substantially over the past decades^{1–4}, and is commonly attributed to increased pollutant emissions from China's rapid economic development^{5,6}. During such episodes, levels of fine particulate matter are harmful to human health and the environment, and cause massive disruption to economic activities^{3,4,7–16}, as occurred in January 2013^{17–21}. Conducive weather conditions are an important ingredient of severe haze episodes^{3,21}, and include reduced surface winter northerlies^{3,21}, weakened northwesterlies in the midtroposphere, and enhanced thermal stability of the lower atmosphere^{1,3,16,21}. How such weather conditions may respond to climate change is not clear. Here we project a 50% increase in the frequency and an 80% increase in the persistence of conducive weather conditions similar to those in January 2013, in response to climate change. The frequency and persistence between the historical (1950–1999) and future (2050–2099) climate were compared in 15 models under Representative Concentration Pathway 8.5 (RCP8.5)²². The increased frequency is consistent with large-scale circulation changes, including an Arctic Oscillation upward trend^{23,24}, weakening East Asian winter monsoon^{25,26}, and faster warming in the lower troposphere^{27,28}. Thus, circulation changes induced by global greenhouse gas emissions can contribute to the increased Beijing severe haze frequency.

Beijing severe haze episodes are most frequent in boreal winter (December, January and February, DJF)^{3,29}, due to high pollutant emissions, and a lack of rain (<11 mm in winter, but >420 mm in summer) to wash away pollutants. The Beijing winter circulation is characterized by northwesterly winds near the surface (Supplementary Fig. 1a) associated with the East Asian winter monsoon, and in the midtroposphere (Supplementary Fig. 1b) associated with the East Asia trough^{3,16,21,30}. During severe haze, the surface and midtropospheric northwesterly winds weaken, or even reverse. The concentration of fine particles with a diameter of 2.5 µm or smaller (PM_{2.5}) increases dramatically. This leads to a sharp decrease in visibility, affecting economic activities by causing air and ground traffic hazards and disruptions^{3,4,16,21}. These fine particles contain toxic substances that affect respiratory and circulatory system, with detrimental impacts on the cardiovascular, immune and nervous systems, arguably increasing morbidity and mortality^{7–12}.

The frequency of Beijing winter severe haze has increased over past decades, culminating in events during January 2013, December 2015 and December 2016, when a high number

of episodes occurred^{16–21}. In January 2013, severe haze events affected 30 cities^{17–21}, and the maximum daily PM_{2.5} average near Beijing reached 500 µg m⁻³. While the underlying cause is increased pollutant emissions, local weather conditions play a part^{3,4,16,21}. Further, decadal variability and change, including weakened northerly winds^{1,30}, decreased relative humidity², reduced Arctic Sea ice⁴, and declined East Asian winter monsoon³⁰, may have contributed. However, no long-term PM_{2.5} observations are available for attribution of the increased frequency.

In particular, how the conducive weather conditions may respond to climate change remains unclear. Climate models forced under the RCP8.5 (high) emission scenario²² simulated a general increase in occurrences of atmospheric stagnation^{27,28}, but no change over Beijing was projected²⁸. Here we show that climate change increases occurrences of weather conditions conducive to Beijing winter severe haze.

Correlation of available observed PM_{2.5} over 2009–2015 with a range of ambient daily anomalies reinforces the link between PM_{2.5} and weather conditions. Strong correlations are found in lower tropospheric meridional flows, midtropospheric zonal flows, and vertical temperature profiles (Supplementary Fig. 2a–c). Defining a severe haze day as one when the concentration of PM_{2.5} > 150 µg m⁻³, we constructed composites of daily meteorological anomalies associated with severe haze, referenced to the daily climatology and normalized by the local standard deviation. We chose the threshold of 150 µg m⁻³ for two reasons. Firstly, this is greater than the observed winter average and median values of 109.7 and 99.3 µg m⁻³, respectively. Secondly, the Beijing municipal government issues a 'red alert' when the PM_{2.5} concentration is forecast to exceed 150 µg m⁻³ for 72 consecutive hours. In the January 2013 episodes, the concentration above 150 µg m⁻³ lasted for four to six days.

The composite vertical temperature profile features warm anomalies in the near-surface (around 850 hPa) preventing vertical dispersion of pollutants, accompanied by an anomalous cooling in the upper atmosphere^{3,21} (Fig. 1a). Guided by location of maximum correlations (Supplementary Fig. 2), the intensity of this thermal structure is measured by a vertical difference (ΔT) in raw temperature anomalies between the near-surface (850 hPa, over the area of 32.5–45° N, 112.5–132.5° E) and the upper atmosphere (250 hPa, 37.5–45° N, 122.5–137.5° E) (green lines in Fig. 1a). These low-level atmosphere warm anomalies are supported by a sea level pressure gradient between a low over China and a high off the east coast^{3,16,21} (Supplementary Fig. 3). This leads to reduced seasonal prevailing surface cold northerlies,

¹Physical Oceanography Laboratory/CIMSST, Ocean University of China and Qingdao National Laboratory for Marine Science and Technology, Yushan Road, Qingdao 266003, China. ²CSIRO Oceans and Atmosphere, Aspendale, Victoria 3195, Australia. ³Institute of Atmospheric Physics, Chinese Academy of Sciences, Beijing 100029, China. ⁴University of Chinese Academy of Sciences, Beijing 100049, China. ⁵School of Environmental Science and Engineering/Joint International Research Laboratory of Climate and Environment Change, Nanjing University of Information Science and Technology, Nanjing 210044, China. ⁶Collaborative Innovation Center on Forecast and Evaluation of Meteorological Disasters/Key Laboratory of Meteorological Disaster of Ministry of Education, Nanjing University for Information Science and Technology, Nanjing 210044, China. *e-mail: hongliao@nuist.edu.cn

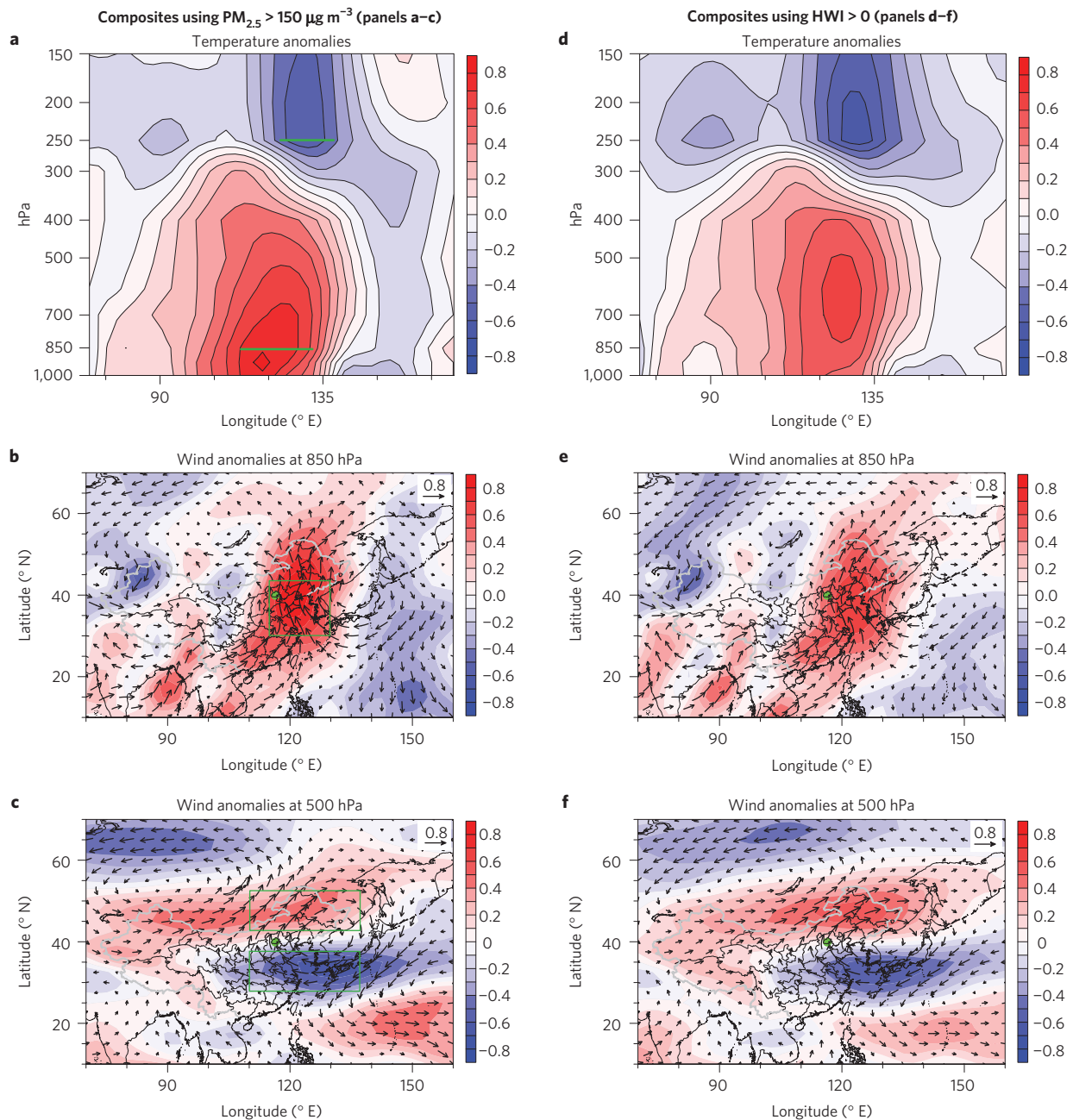


Figure 1 | Observed Beijing (116.4° E, 39.9° N) winter severe haze weather conditions and their representation by a haze weather index (HWI).

a, Composites of days with observed $PM_{2.5} > 150 \mu g m^{-3}$ over the 7-year period (2009–2015; also see Fig. 2), for anomalous temperatures throughout the atmospheric column in an east–west section. **b**, Anomalous wind vectors at 850 hPa. Shading indicates meridional flow. **c**, Anomalous wind vectors at 500 hPa. Shading indicates zonal flow. Reanalysis data is used for wind anomalies (see Methods). Shown are anomalies referenced to the mean over 1986–2015 and normalized by the local standard deviation for the period. **d–f**, The same as in **a–c**, respectively, but using $HWI > 0$. The green dot denotes the location of Beijing. Green boxes/lines denote regions for averages.

or increased occurrences of near-surface southerlies from the south of Beijing, referred to as V850, averaged over the broader Beijing area (30°–47.5° N, 115°–130° E; green box in Fig. 1b). Conducive to warming and increased moisture, the southerlies are favourable for haze formation and maintenance. In the midtroposphere, the East Asia trough shallows during severe haze, and the associated northwesterlies extend to the north rather than south of Beijing^{3,4}, weakening the cold and dry northwesterly flows to Beijing and reducing the wind speed (Fig. 1c). This is unfavourable for horizontal dispersion of pollutants out of Beijing. The weakened midtropospheric flow may be measured by a latitudinal difference in 500 hPa zonal winds north of Beijing (42.5–52.5° N, 110–137.5° E)

minus the average over south of Beijing (27.5–37.5° N, 110–137.5° E; green boxes in Fig. 1c), hereafter denoted as U500. A positive U500 indicates weakening northwesterly flows to Beijing.

These features form a basis for establishing a relationship between Beijing winter daily $PM_{2.5}$ (black curve, Fig. 2) and meteorological anomalies. We also examined a suite of other relevant variables, including geopotential height, boundary layer thickness and local stratification instability^{3,4,16,21} (Supplementary Figs 3 and 4), but their regional averages are not as highly correlated with $PM_{2.5}$. A multiple linear regression model also identifies V850, ΔT and U500 as the dominant variables. However, these three variables are not independent; detrended DJF daily V850, ΔT and

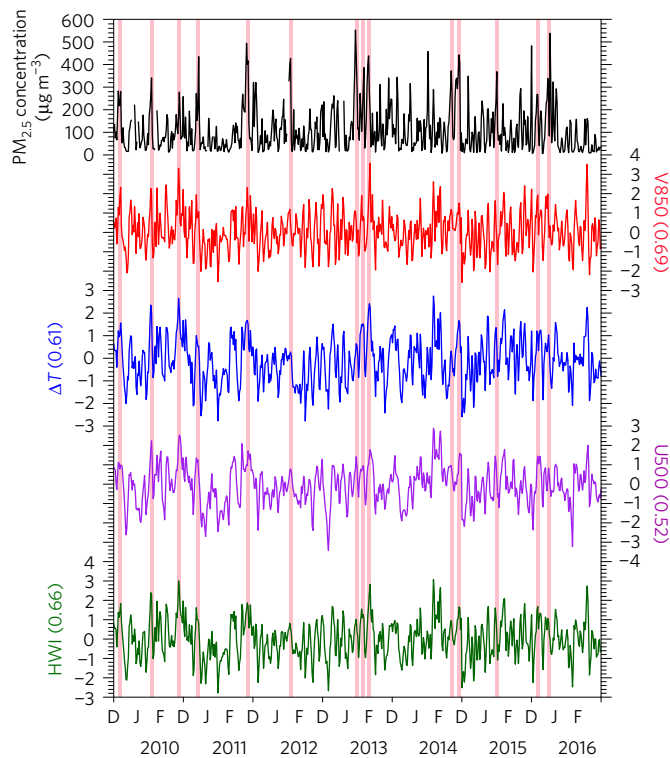


Figure 2 | Time series of 2009–2015 normalized observed boreal winter daily $PM_{2.5}$ ($\mu\text{g m}^{-3}$) and normalized daily weather conditions near Beijing. V850 (red), ΔT (blue) and U500 (purple) (see text for their definitions) are normalized by their respective standard deviations. Occurrences when $PM_{2.5}$ reached a high concentration are highlighted. Highlighted slots illustrate the correlations between weather time series, and with $PM_{2.5}$ as listed in brackets near the y-axis labels. The haze weather index (HWI; green) is constructed by adding the above three weather time series, and scaling by the standard deviation of the combined time series.

U500 are correlated (red, blue, purple, Fig. 2) with correlation coefficients over the 1986–2015 period in the range of 0.69–0.80, and are in turn correlated with the other daily variables listed above. Thus, favourable weather conditions co-occur to provide a conducive setting for severe haze events.

Because V850, ΔT and U500 are not independent, we normalized each time series by its respective standard deviation and summed the three normalized time series to construct a single index. The new index was again normalized by its standard deviation, and is referred to as haze weather index (HWI; green, Fig. 2). The correlation between $PM_{2.5}$ and the HWI is 0.66. Adding more weather variables virtually does not change the correlation, because the effect of the other variables is implicitly included in the HWI by being related to the three dominant variables.

The HWI is effective in representing the conducive weather conditions. Within the seven-year $PM_{2.5}$ observations, there are 164 winter severe haze days with $PM_{2.5} > 150 \mu\text{g m}^{-3}$, out of which there are 146 days with $HWI > 0$ and 72 days with $HWI > 1$. Thus, 89% (146/164) of all observed severe haze events occurred with a $HWI > 0$. By contrast, only 28% of severe haze events were captured by a winter atmosphere stagnation index based on ref. 28. Over the seven years, there are 303 days with $HWI > 0$ and 103 days with $HWI > 1$ days. That is, 48% (146/303) of the $HWI > 0$ days, and 70% (72/103) of the $HWI > 1$ days, are severe haze days (Supplementary Figs 5 and 6). The percentage increases with the HWI value. The HWI averaged over the severe haze events of January 2013 is 1.02, reinforcing the importance of conducive weather conditions.

To further demonstrate the power of our index, we construct daily composites of meteorological conditions over all days with $HWI > 0$ and compare them to the $PM_{2.5} > 150 \mu\text{g m}^{-3}$ composites using normalized anomalies (see Methods). Composites for days with $HWI > 0$ (Fig. 1d–f) resemble those for days with $PM_{2.5} > 150 \mu\text{g m}^{-3}$ (Fig. 1a–c).

The frequency of the conducive weather conditions, as measured by the winter HWI, has increased since 1948. From the first half (1948–1981) to the second (1982–2015) half of the 1948/1949–2015/2016 period (Supplementary Fig. 7), there is an increase of 10% in the mean frequency of $HWI > 0$ occurrences, from 45.5 days to 50.2 days per season. The increased frequency is statistically significant above the 99% confidence level, but the role of climate change is not clear.

We assess the role of climate change by comparing the frequency of the winter conducive weather conditions between the historical 50-year (1950–1999) and the future 50-year climate (2050–2099) in 15 CMIP5 models²² for which daily data are available. These experiments are forced by historical emissions before 2006, and under the RCP8.5 (high emission) scenario over 2006–2100. To construct the historical HWI index, daily V850, ΔT and U500 are constructed using daily anomalies referenced to the historical 50-year daily mean, and normalized by the historical standard deviation. The properties of modelled historical HWI compare well with the observed (Supplementary Tables 1 and 2). To facilitate a meaningful comparison, for the future HWI index, daily anomalies are referenced to the same historical daily climatology and normalized by the same historical standard deviation.

Under climate change, the frequency of conducive weather conditions increases markedly, manifested as a systematic shift towards higher HWI values (Fig. 3a), contributed by a similar shift towards a higher frequency of weaker northerly winds, more stable lower atmosphere conditions, and weaker East Asia troughs (Fig. 3b–d). Aggregated over the 15 models, there is a 20% increase in days with $HWI > 0$; a more than 50% increase in days with $HWI > 1$, the conditions under which the January 2013 events occurred; and a 131% increase in days with $HWI > 2$ (Supplementary Table 3).

These results are supported by a strong inter-model consensus, with 14 out of 15 models producing increased frequency in days with $HWI > 0$ (Supplementary Table 1). The increase is statistically significant above the 95% confidence using a bootstrap method (Supplementary Table 4; see Methods), or when more variables are included (Supplementary Table 5).

Composite patterns of future conducive anomalies, referenced to the historical climatology and normalized by the historical standard deviation, for $HWI > 0$ days show strong similarity between the historical (Fig. 4a–c) and future climate (Fig. 4d–f). There is little change in the average intensity (Supplementary Fig. 8), suggesting that the conducive weather conditions simply occur more frequently. The frequency of conducive weather conditions of $HWI > 1$ persisting for several consecutive days increases markedly; for example, the frequency of events with persistence of four days or longer, as occurred in January 2013, increases from 1 event to 1.8 events per year, an 80% increase (Supplementary Fig. 9).

The increased frequency of conducive weather conditions is consistent with the mean state changes affecting the Beijing region. Firstly, the near-surface atmosphere warms faster leading to a more stable atmosphere^{27,28}. Secondly, land warms faster than the ocean, leading to a weakened East Asian winter monsoon and reduced surface and midtropospheric northwesterlies (Fig. 5a,b). This is supported by a shallowing in the East Asia trough^{25,26} (Fig. 5c,d), manifested as a northward and eastward shift, making weather events with cool and dry northwesterlies more difficult to extend to Beijing^{3,4}. Near the surface, mean sea level pressure decreases near the pole but increases in the mid-latitudes, a pattern referred to

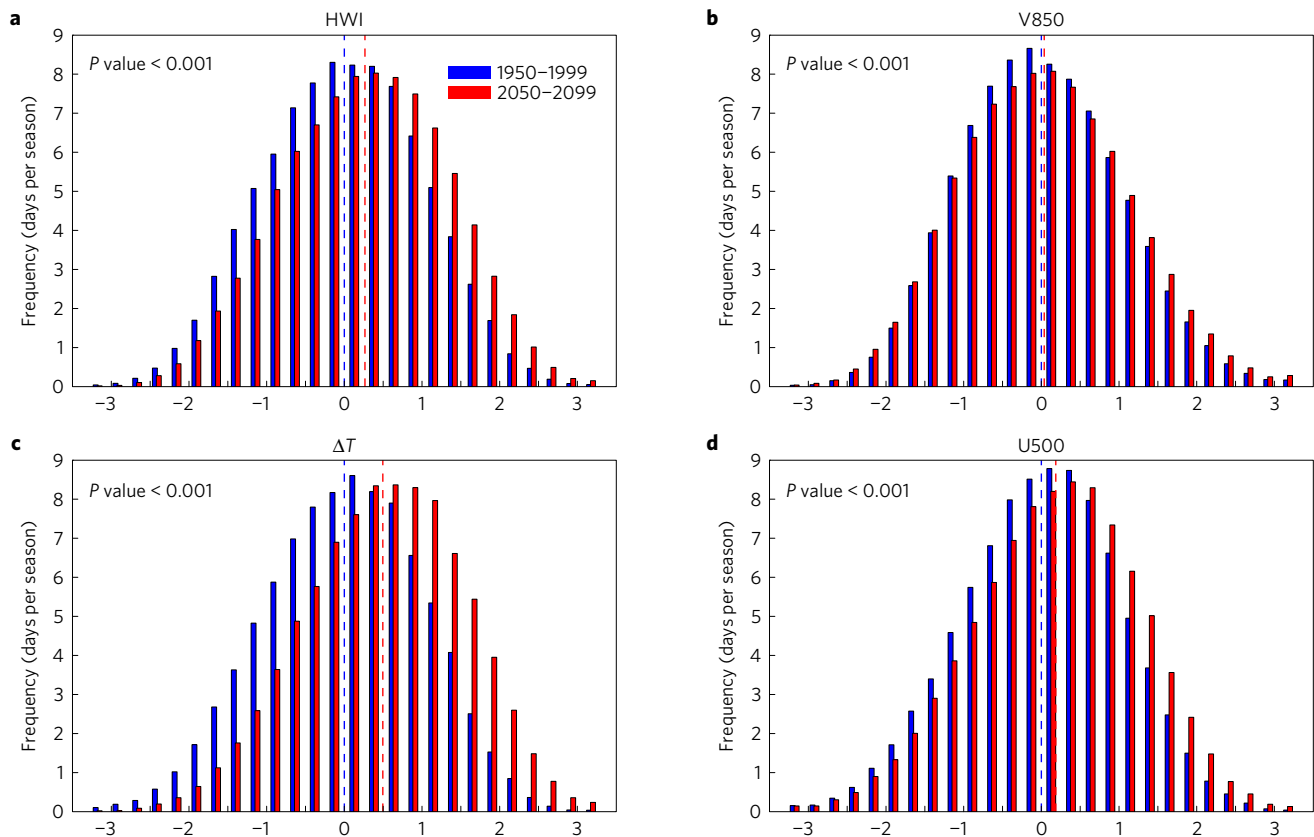


Figure 3 | Future changes of Beijing winter severe haze weather conditions based on climate models. **a**, Histograms of historical (blue bars, 1950–1999) and future (red bars, 2050–2099) haze weather index (HWI), aggregated from 15 climate models under historical emissions and future emission scenario RCP8.5 (ref. 22). The HWI is constructed referenced to the historical winter daily climatology and normalized by the historical standard deviation for both periods. **b–d**, The same as **a**, but for the three contributing components, V850 (**b**), ΔT (**c**) and U500 (**d**). The histograms show that for a given threshold, there is an increased frequency of weather conditions conducive to severe haze events in the future.

as the positive phase of the Arctic Oscillation. This pattern trends upward under climate change^{23,24}, and the high pressure centre over the North Pacific (Supplementary Fig. 10) embedded in the pattern is conducive to weakening of near-surface northerlies over Beijing. These factors conspire to generate an increased frequency of conducive weather conditions.

In summary, the frequency and persistence of weather conditions conducive to Beijing winter severe haze events are projected to increase substantially under climate change. The increase is consistent with mean state changes, which include a faster warming in the lower atmosphere, weakening of the East Asia winter monsoon, shallowing of the East Asia trough, and rising mid-latitude mean sea level pressures over the North Pacific Ocean embedded in the upward trend of the Arctic Oscillation. We note that $PM_{2.5}$ observations cover only seven years and might not identify all conducive weather conditions. Sustainable observations, with data made publicly available to facilitate further research, are needed. Our results nevertheless suggest that circulation changes induced by global greenhouse gas emissions can play an important role. Global effort in reducing greenhouse gas emissions will contribute to decreasing the risk of Beijing winter severe haze events.

Methods

Methods, including statements of data availability and any associated accession codes and references, are available in the [online version of this paper](#).

Received 6 July 2016; accepted 6 February 2017;
published online 20 March 2017

References

- Niu, F., Li, Z. Q., Li, C., Lee, K. H. & Wang, M. Y. Increase of wintertime fog in China: potential impacts of weakening of the eastern Asian monsoon circulation and increasing aerosol loading. *J. Geophys. Res.* **115**, D00K20 (2010).
- Ding, Y. H. & Liu, Y. J. Analysis of long-term variations of fog and haze in China in recent 50 years and their relations with atmospheric humidity. *Sci. China Earth Sci.* **57**, 36–46 (2014).
- Chen, H. & Wang, H. Haze days in north China and the associated atmospheric circulations based on daily visibility data from 1960 to 2012. *J. Geophys. Res.* **120**, 5895–5909 (2015).
- Wang, H. J., Chen, H. P. & Liu, J. Arctic sea ice decline intensified haze pollution in eastern China. *Atmos. Ocean. Sci. Lett.* **8**, 1–9 (2015).
- Guo, J. *et al.* Spatiotemporal variation trends of satellite-based aerosol optical depth in China during 1980–2008. *Atmos. Environ.* **45**, 6802–6811 (2011).
- Zhou, Y. *et al.* The impact of transportation control measures on emission reductions during the 2008 Olympic Games in Beijing, China. *Atmos. Environ.* **44**, 285–293 (2010).
- Bai, N., Khazaei, M., van Eeden, S. F. & Laher, I. The pharmacology of particulate matter air pollution-induced cardiovascular dysfunction. *Pharmacol. Ther.* **113**, 16–29 (2007).
- Kan, H. *et al.* Differentiating the effects of fine and coarse particles on daily mortality in Shanghai, China. *Environ. Int.* **33**, 376–384 (2007).
- Araujo, J. A. *et al.* Ambient particulate pollutants in the ultrafine range promote early atherosclerosis and systemic oxidative stress. *Circ. Res.* **102**, 589–596 (2008).
- Pope, C. A. III & Dockery, D. W. Health effects of fine particulate air pollution: lines that connect. *J. Air. Waste Manage. Assoc.* **56**, 709–742 (2006).
- Wang, X. P. & Mauzerall, D. L. Evaluating impacts of air pollution in China on public health: implications for future air pollution and energy policies. *Atmos. Environ.* **40**, 1706–1721 (2006).
- Xu, P., Chen, Y. F. & Ye, X. J. Haze, air pollution, and health in China. *Lancet* **382**, 2067 (2013).
- Qian, Y., Leung, L. R., Ghan, S. J. & Giorgi, F. Regional climate effects of aerosols over China: modeling and observation. *Tellus B* **55**, 914–934 (2003).

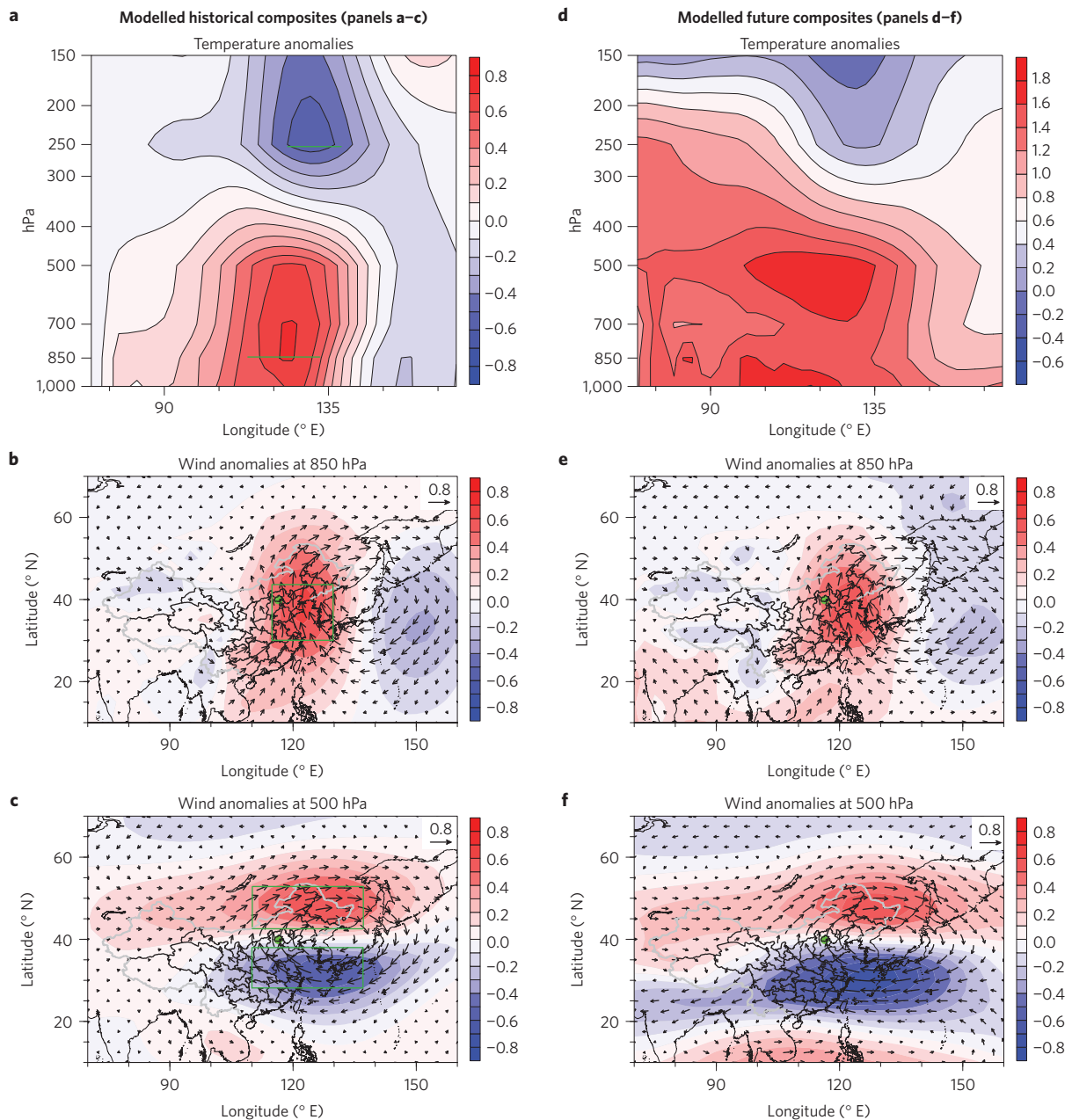


Figure 4 | Simulated winter severe haze weather conditions near Beijing (116.4° E, 39.9° N). a–c, Composites for days with HWI > 0 in terms of anomalous temperatures throughout the atmospheric column in an east–west section (**a**), anomalous flow vectors at 850 hPa for V850 (shading indicates meridional flow) (**b**), and anomalous flows at 500 hPa for U500 (shading indicates zonal flow) (**c**), for the historical climate (1950–1999). **d–f**, The same as **a–c**, respectively, but for future climate (2050–2099), aggregated over 15 models. All anomalies are referenced to the historical daily climatology and normalized by the historical standard deviation to facilitate comparison between the historical and future climate. The green dot denotes the location of Beijing. The green boxes denote regions for averages.

- Liao, H., Chang, W. Y. & Yang, Y. Climatic effects of air pollutants over China: a review. *Adv. Atmos. Sci.* **32**, 115–139 (2015).
- Li, Z. *et al.* East Asian studies of tropospheric aerosols and their impact on regional climate (EAST-AIRC): an overview. *J. Geophys. Res.* **116**, D00K34 (2011).
- Li, Q., Zhang, R. & Wang, Y. Interannual variation of the wintertime fog–haze days across central and eastern China and its relation with East Asian winter monsoon. *Int. J. Climatol.* **36**, 346–354 (2016).
- Huang, R. J. *et al.* High secondary aerosol contribution to particulate pollution during haze events in China. *Nature* **514**, 218–222 (2014).
- Ji, D. *et al.* The heaviest particulate air-pollution episodes occurred in northern China in January, 2013: insights gained from observation. *Atmos. Environ.* **92**, 546–556 (2014).
- Quan, J. *et al.* Characteristics of heavy aerosol pollution during the 2012–2013 winter in Beijing, China. *Atmos. Environ.* **88**, 83–89 (2014).
- Yang, Y. *et al.* Formation mechanism of continuous extreme haze episodes in the megacity Beijing, China, in January 2013. *Atmos. Res.* **155**, 192–203 (2015).
- Zhang, R. H., Li, Q. & Zhang, R. N. Meteorological conditions for the persistent severe fog and haze event over eastern China in January 2013. *Sci. China Earth Sci.* **57**, 26–35 (2014).
- Taylor, K. E., Stouffer, R. J. & Meehl, G. A. An overview of CMIP5 and the experiment design. *Bull. Am. Meteorol. Soc.* **93**, 485–498 (2012).
- Shindell, D. T. *et al.* Simulation of recent northern winter climate trends by greenhouse-gas forcing. *Nature* **399**, 452–455 (1999).
- Fyfe, J. C., Boer, G. J. & Flato, G. M. The Arctic and Antarctic oscillations and their projected changes under global warming. *J. Geophys. Res.* **26**, 1601–1604 (1999).
- Hori, M. E. & Ueda, H. Impact of global warming on the East Asian winter monsoon as revealed by nine coupled atmosphere–ocean GCMs. *Geophys. Res. Lett.* **33**, L03713 (2006).

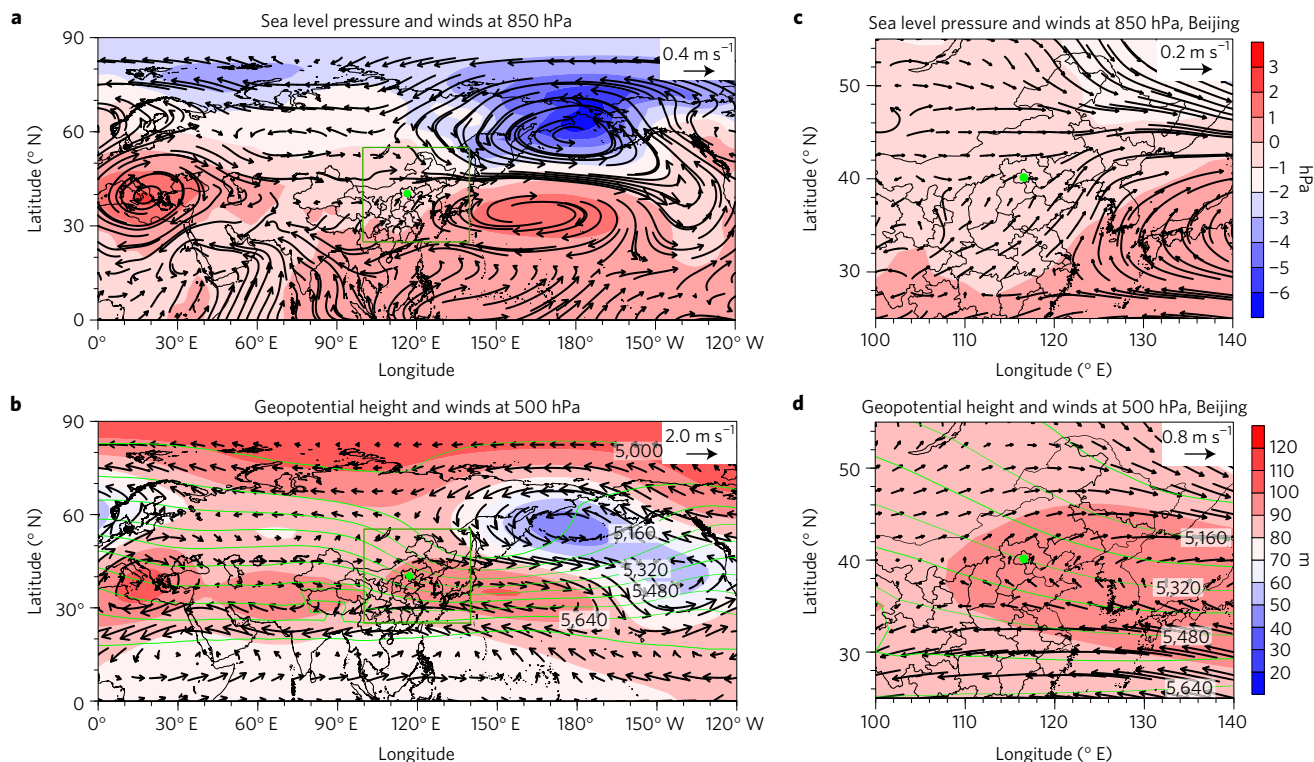


Figure 5 | Simulated multi-model ensemble mean state changes in boreal winter mean circulation. a, b, Changes in 850 hPa wind vectors (m s^{-1}) and sea level pressure (hPa) (**a**), and 500 hPa wind vectors (m s^{-1}) and 500 hPa geopotential height (m) (**b**). These changes are taken as the difference between the future and the historical climate (2050–2099 minus 1950–1999). **c, d**, The same as **a, b**, respectively, but with a focus on the Beijing area. These changes are consistent with an upward trend of the Arctic Oscillation and a weakening East Asia winter monsoon, both contributing to anomalous southerly winds near Beijing. Green contours in **b** and **d** are simulated mean 500 hPa geopotential height (m) under the historical climate (1950–1999). The green boxes denote regions for focus in **c** and **d**.

26. Xu, M., Xu, H. & Ma, J. Responses of the East Asian winter monsoon to global warming in CMIP5 models. *Int. J. Climatol.* **36**, 2139–2155 (2016).
27. Jacob, D. J. & Winner, D. A. Effect of climate change on air quality. *Atmos. Environ.* **43**, 51–63 (2009).
28. Horton, D. E., Skinner, C. B., Singh, D. & Diffenbaugh, N. S. Occurrence and persistence of future atmospheric stagnation events. *Nat. Clim. Change* **4**, 698–703 (2014).
29. Zhang, R. *et al.* Chemical characterization and source apportionment of $\text{PM}_{2.5}$ in Beijing: seasonal perspective. *Atmos. Chem. Phys.* **13**, 7053–7074 (2013).
30. Xu, M. *et al.* Steady decline of East Asian monsoon winds, 1969–2000: evidence from direct ground measurements of wind speed. *J. Geophys. Res.* **111**, D24111 (2006).

Acknowledgements

W.C. is supported by a Greencard Professor of the Ocean University of China, the Australian Climate Change Science Program, and a CSIRO Office of Chief Executive Science Leader award. H.L. is supported by the National Basic Research Program of

China (973 program, Grant No. 2014CB441202) and the National Natural Science Foundation of China under grant 91544219.

Author contributions

W.C. and H.L. conceived the study. W.C. and H.L. directed the analysis, and W.C. wrote the first draft of the paper with K.L. K.L. performed the analysis. All authors contributed to interpreting results, discussion of the associated dynamics, and improvement of this paper.

Additional information

Supplementary information is available in the online version of the paper. Reprints and permissions information is available online at www.nature.com/reprints. Publisher's note: Springer Nature remains neutral with regard to jurisdictional claims in published maps and institutional affiliations. Correspondence and requests for materials should be addressed to H.L.

Competing financial interests

The authors declare no competing financial interests.

Methods

Data. We utilized daily fields, such as surface winds, mean sea level pressure, and midtropospheric winds from the National Center for Environmental Prediction (NCEP) and National Center for Atmospheric Research (NCAR) global reanalysis³¹, at a resolution of 2.5° latitude by 2.5° longitude. Beijing severe haze events occur more frequently in boreal winter (December, January and February; DJF) than in other seasons^{32,39}. We focused on the winter occurrences. We constructed a winter daily climatology, and obtained normalized daily anomalies by referencing to the daily climatology and scaling them by the standard deviation. We used a seven-year observed time series of PM_{2.5} in Beijing (117° E, 40° N), commencing in 2009, available from the US Embassy and from the following website (<http://www.stateair.net/web/historical/1/1.html>). This time series has been used in many studies^{32–36}, which have demonstrated strong consistency with other observations or proxies of PM_{2.5}.

Linkage between severe haze events and weather conditions. To examine the weather linkage, we concatenated the seven years of winter daily PM_{2.5} (632 samples), and correlated them with similarly arranged time series of anomalies. The correlation maps for vertical temperatures, near-surface winds, midtropospheric winds, and other weather parameters show a strong linkage of PM_{2.5} to weather conditions (Supplementary Figs 2–4). The patterns illustrate the role of a stable lower atmosphere (measured by ΔT), weaker near-surface northerlies (referred to as V850), and weaker midtropospheric northwesterlies (denoted as U500). Positive values indicate a condition conducive to high PM_{2.5}.

To confirm the role of these circulation anomalies, we conducted a composite analysis. We defined a severe haze event as when daily average PM_{2.5} reaches a threshold value of 150 $\mu\text{g m}^{-3}$. There are 164 days of PM_{2.5} > 150 $\mu\text{g m}^{-3}$ during the last seven winters, that is, an average 23.4 days per season. This is a more direct definition compared with previous studies in which visibility less than 10 km and relative humidity less than 90% are used^{5,21}. Patterns of composite anomalies strengthen the notion that severe haze events tend to occur in favourable weather conditions. We also tested sensitivity to different thresholds, for example, PM_{2.5} > 200 $\mu\text{g m}^{-3}$, and found that the anomaly patterns are similar and the intensity greater. Due to the limited observations (2009–2015), the cause for the observed changes of severe haze days over the past seven years is not clear.

Haze weather index (HWI) and its observed change. Other daily meteorological anomalies, such as geopotential height, sea level pressure, relative humidity (Supplementary Fig. 3), near-surface wind speed, boundary layer thickness, and local stratification instability^{3,4,21} (Supplementary Fig. 4), are also involved, but these are not independent variables. For example, the detrended time series of DJF daily ΔT , V850 and U500 are correlated (Fig. 2), with correlation coefficients over the 1986–2015 period (30 × 90 days, discarding 29 February) ranging between 0.69 and 0.80, and these three time series are also correlated with the other daily anomalies. To simplify analysis and considering a lack of model daily fields available for calculating (for example, boundary layer thickness), we chose the three time series that provide the highest correlation (ΔT , V850 and U500). We tested the sensitivity of the HWI to the inclusion of more weather parameters, for example, a local stratification instability^{3,4,21}, and found little differences by including more parameters. The correlation between the HWI and a time series of visibility over Beijing is -0.64 over the 2009–2014, and -0.61 over the 1982–2014 period.

The local stratification instability is commonly indicated by a K index, which is derived by the following formulation: $K = (T_{850} - T_{500}) + T_{d850} - (T - T_d)_{700}$, where T_j is air temperature at pressure level j (hPa), and $(T_d)_j$ is dew point temperature at pressure level j (hPa)²¹. The K index indicates the stratification instability in the lower and middle atmosphere. The larger the stratification instability and the inversion are, the stronger the haze event. The smaller the dew point deficit is, the stronger the haze is²¹. Including a K index averaged over Beijing improves the correlation between PM_{2.5} and HWI only marginally.

The severe haze weather conditions, ΔT , V850 and U500, and parameters such as mean sea level and relative humidity, are not independent from each other, but are correlated. As such, we normalized the ΔT , V850 and U500 time series by their respective standard deviation (Fig. 2), and combined them into one index by summing the three normalized time series. The new index is then normalized by its standard deviation, and is referred to as a HWI (Fig. 2). A positive index value means that it is conducive to severe haze events. Applying this procedure to NCEP/NCAR³¹ boreal winter daily anomalies over the 1948–2015 period shows that the frequency over the second half of the period (50.2 days per season) is

higher than that over the first half (45.5 days per season) (Supplementary Fig. 7). However, whether climate change plays a part is not clear.

CMIP5 experiments. To examine how the conducive weather conditions will respond to greenhouse warming, we assessed 15 CMIP5 models (Supplementary Table 1)²², in which daily outputs are available covering historical and future climate. As similar with construction of the HWI using the NCEP data, time series of the HWI for the historical and future winter are established and we compared their histograms (Fig. 3). All of the reanalysis and CMIP5 data are interpolated to a common resolution of 2.5° × 2.5°.

Model sea level pressure trends. To examine the trend of sea level pressures in each model, we applied empirical orthogonal function³⁷ analysis to boreal winter anomalies, referenced to the historical climatology, in the domain of 0° northward from 1950 to 2100. The first mode features a spatial pattern with anomalously high sea level pressure in the mid-latitudes but low sea level pressure in the high latitudes, referred to as the positive phase of the Arctic Oscillation^{23,24}. The mid-latitude pressure is not spatially uniform but shows a local high pressure centre over the North Pacific (Supplementary Fig. 10a), supporting anomalous southerly winds near Beijing. This pattern trends upwards in 14 of the 15 models (Supplementary Fig. 10), contributing to decreasing northerly winds over Beijing.

Statistical significance and sensitivity to inclusion of more weather parameters. We use a bootstrap method³⁸ to examine whether the difference in frequency of the conducive weather conditions in the CMIP5 historical and future climate is statistically significant. There are a total of 67,500 days of HWI for the historical climate from 15 CMIP5 models (15 models × 50 years × 90 days). For the bootstrap test, the 67,500 samples in the historical climate were re-sampled randomly to construct another 10,000 realizations of 67,500-year records. In the random re-sampling process, any HWI value is allowed to be selected again. The standard deviation of the HWI > 0 frequency in the inter-realization is 0.33 days per season. The same procedure is carried out for the future climate period and the standard deviation of the HWI > 0 frequency in the inter-realization is 0.38 days per season. The sum of these uncertainty values (0.71 days per season) is far smaller than the difference of 8.7 days per season between the historical and future climate (Fig. 3a and Supplementary Table 1), indicating strong statistical significance of our result (99.9% confidence level). Increasing the realizations to 20,000 or 30,000 yields essentially an identical result. The same test is carried out for HWI > 0.5, 1, 2, and for all contributing components (see Supplementary Table 4).

We tested the sensitivity of HWI change to the inclusion of local stratification instability (that is, K index²¹) in the construction of the HWI. The multi-model mean change in the HWI produces only a small increase for most of the HWI thresholds when compared with the case without the K index (Supplementary Tables 3 and 5).

Data availability. All data supporting the findings of this study are available from the corresponding author on request.

References

- Kalnay, E. *et al.* The NCEP/NCAR 40-year reanalysis project. *Bull. Am. Meteorol. Soc.* **3**, 437–471 (1996).
- Jiang, J. *et al.* Particulate matter distributions in China during a winter period with frequent pollution episodes (January 2013). *Aerosol Air Qual. Res.* **15**, 494–503 (2015).
- Mukherjee, A. & Toohy, D. W. A study of aerosol properties based on observations of particulate matter from the US Embassy in Beijing, China. *Earth's Future* **4**, 381–395 (2016).
- San Martini, F. M., Hasenkopf, C. A. & Roberts, D. C. Statistical analysis of PM2.5 observations from diplomatic facilities in China. *Atmos. Environ.* **110**, 174–185 (2015).
- Wang, J. F., Hu, M. G., Xu, C. D., Christakos, G. & Zhao, Y. Estimation of air citywide pollution in Beijing. *PLoS ONE* **8**, e53400 (2013).
- Zheng, S., Pozzer, A., Cao, C. X. & Lelieveld, J. Long-term (2001–2012) concentrations of fine particulate matter (PM2.5) and the impact on human health in Beijing, China. *Atmos. Chem. Phys.* **15**, 5715–5725 (2015).
- Lorenz, E. N. *Empirical Orthogonal Functions and Statistical Weather Prediction* Statistical Forecast Project Report 1 (MIT Department of Meteorology, 1956).
- Austin, P. C. Bootstrap methods for developing predictive models. *Am. Stat.* **58**, 131–137 (2004).